

Exact non-equilibrium transport through point contacts in quantum wires and fractional quantum Hall devices

P. Fendley¹, A.W.W. Ludwig^{2†} and H. Saleur^{1*}

¹ Department of Physics, University of Southern California
Los Angeles CA 90089-0484

² Department of Physics, University of California
Santa Barbara CA 93106

We have recently calculated exact non-equilibrium quantum transport properties through a point contact in a Luttinger liquid. Using a particular quasiparticle basis of the Hilbert space dictated by integrability, we here compute explicitly the exact $I(V)$ characteristic and conductance *out of equilibrium* as a function of driving voltage V and temperature T . These are described by universal scaling functions of two variables, the scaled point-contact interaction strength, and V/T . The differential-conductance curve as a function of the interaction strength broadens significantly as V/T is increased, and develops a pronounced maximum at a (universal) critical value $(eV/k_B T) = 7.18868\dots$. In addition, we derive an exact duality between strong and weak backscattering. The theory presented here has recently been realized experimentally in resonant tunneling-transport experiments between edge states in fractional quantum Hall effect devices. In this context the exact duality is between electron tunneling and Laughlin-quasiparticle tunneling.

[†] A.P. Sloan Fellow

* Packard Fellow

1. Introduction

Non-equilibrium quantum transport in fully-interacting systems is a barely-explored territory of theoretical physics. Equilibrium statistical mechanics of interacting systems, on the other hand, can sometimes be studied reliably by using powerful field-theoretical techniques (including conformal field theory and the Bethe ansatz). Bethe-ansatz integrability is useful in equilibrium even in the absence of scale invariance, permitting one to study the exact crossover behavior between critical points. However, integrability has for the most part been useful for calculating only thermodynamic quantities, excluding correlation functions and transport at non-zero temperature. However, by using the “quasi-particle approach” to integrability, we have recently shown that, quite unexpectedly, one *can* compute exact transport properties through a point contact, even out of equilibrium [1]. Here we discuss non-equilibrium transport through point contacts in a Luttinger liquid. This model is realized in resonant tunneling experiments through point contacts in quantum Hall effect devices [2].

The key observation in [1] was that (i) tunneling is integrable and that (ii) integrability defines a quasiparticle basis of the Hilbert space of the leads which is particularly suited to computing transport. In this basis, scattering processes at the point contact proceed without particle production. These quasiparticles are not free. However, their interactions can be incorporated exactly into *non-fermi distribution functions*, which govern the filling of single-particle levels (orbitals) with quasiparticles in the thermodynamic limit. Even though these distribution functions are not that of Fermi-Dirac, in an integrable model they can be computed exactly using thermodynamic Bethe ansatz (TBA) technology. Once this quasiparticle basis arising from integrability has been identified, non-equilibrium transport properties such as the exact $I(V)$ curve and the conductance through the point contact can be computed exactly using a kinetic (Boltzmann) equation for these quasiparticles. This is possible even though the point-contact interaction is non-Gaussian, because the constraints of integrability give the exact S matrix of transmission and reflection amplitudes for these quasiparticles scattering off the point contact. This elastic single-quasiparticle S matrix is momentum-dependent, and, since there is no quasiparticle production in this basis, it is unitary. The S -matrix for scattering of a multi-particle state off the contact factorizes into a product of single particle S -matrices. This means that reflection and transmission processes of single quasiparticles by the point contact occur successively (“one-by-one”), and are the only scattering events. Therefore, these single quasiparticle processes describe the effect of the point-contact interaction fully and exactly.

The purpose of this paper is threefold: (i) We give the details of our exact non-equilibrium transport calculations through point contacts, using Bethe ansatz integrability. We have recently reported briefly on some of our results in [1]. (ii): We give universal explicit curves for the $I(V)$ characteristic and the conductance of those point contact devices, for all temperatures, for comparison with future experiments. (iii): We prove the existence of an exact duality symmetry in this interacting system between weak and strong backscattering. In the context of the quantum Hall effect this corresponds to a duality between electron tunneling and Laughlin-quasiparticle tunneling.

The Luttinger model is one of the simplest non-fermi-liquid metals [3]. It consists of left- and right-moving gapless excitations at the two fermi points in an interacting 1-dimensional electron gas. In the past, this model had been difficult to realize experimentally. This is simply because in a one-dimensional conductor (such as a quasi-one-dimensional quantum wire so thin that the transverse modes are frozen out at low temperature), random impurities occur in the fabrication process. These impurities lead to localization due to backscattering processes between the excitations at the two fermi points. In other words, the random impurities generate a mass gap for the fermions. However, the edge excitations at the boundary of samples prepared in a fractional quantum Hall state should be extremely clean realizations of the Luttinger non-fermi liquids [4]. These are stable because for $1/\nu$ an odd integer, the excitations only move in one direction on a given edge. Since the right and left edges are far apart from each other, backscattering processes due to random impurities in the bulk cannot localize those extended edge states. Moreover, the Luttinger interaction parameter is universally related to the filling fraction ν of the quantum Hall state in the bulk sample by a topological argument based on the underlying Chern-Simons theory, and does therefore not renormalize. The edge states should therefore provide an extremely clean experimental realization of the Luttinger model.

We study the tunneling conductance through a local backscattering potential in the Luttinger model, which gives a fingerprint of the non-fermi liquid state in the Luttinger metal. This situation is realized in resonant tunneling experiments through a point contact in $\nu = 1/3$ quantum Hall devices [4,5,6]. The point contact causes backscattering between right- and left-moving edge excitations, but since the coupling is only at a point, it can be controlled experimentally (and theoretically). The tunneling conductance can thus be viewed as a spectroscopy of the Luttinger non-fermi-liquid state in the quantum Hall edges. Indeed, the experimentally-measured linear-response conductance agrees remarkably well with our exact predictions based on the Luttinger model [1]. This appears to provide

very convincing evidence that the Luttinger model describes the edge state in fractional quantum Hall devices.

In this paper we study non-equilibrium transport through such an impurity in detail. Studying transport properties is crucial for making contact with experiment; thermodynamic properties such as the specific heat arising from a point contact are clearly not accessible experimentally. In the quantum Hall experiments one uses a 4-terminal geometry of the quantum Hall bar, which is long in the x -direction and short in the y -direction. The left-moving (upper) edge of the Hall bar is connected to battery on the right such that the charge carriers are injected into the left-moving lead of the Hall bar with an equilibrium thermal distribution at chemical potential μ_L . Similarly, the right-moving carriers (propagating in the lower edge) are injected from the left, with a thermal distribution at chemical potential μ_R . The difference of chemical potentials of the injected charge carriers is the driving voltage $V = \mu_L - \mu_R$. If $V > 0$, there are more carriers injected from the right than from the left, and a “source-drain” current flows from the right to the left, along the x -direction of the Hall bar. In the absence of the point contact, the driving voltage places the right and left edges at different potentials (in the y -direction, perpendicular to the current flow), implying that the ratio of source-drain current to the driving voltage V is the Hall conductance.

In the absence of any point-contact interaction, the source-drain current $I_0(V)$ may be computed in a variety of ways (see e.g. [7,5]). The resulting conductance is $\nu e^2/h$ (in linear response and at finite driving voltage V). When we include a point-contact interaction at finite driving voltage, more of the left-moving carriers injected from the right are backscattered than those injected from the left, resulting in a loss of charge carriers from the source-drain current. In this case we write the total source-drain current as $I(V) = I_0(V) + I_B(V)$, where $I_B(V)$ is the (negative) backscattering current, quantifying the loss of current due to backscattering at the point contact. It is this backscattering current which we compute exactly here, for finite driving voltage V and all temperatures T . This computation is possible since backscattering does not deplete the (infinite) right and left reservoirs (the battery), so that we can use the individual thermal distribution functions for the left and right reservoirs.

The $I(V)$ characteristic as well as the conductance are described by three parameters, V , T and T_B , where T_B (analogous to the Kondo temperature in the Kondo effect) is a measure of the point contact interaction strength. However, due to the underlying quantum critical point, these observables are described by universal scaling functions of two

ratios, the scaled interaction strength T_B/T , and V/T . We display the exact differential conductance $G(T_B/V, V/T) \equiv \frac{\partial I(V)}{\partial V}$ in fig. 1. As apparent from fig. 1, an interesting prediction of our exact solution is that the differential conductance exhibits a pronounced maximum as a function of the point contact interaction strength, whenever the ratio V/T exceeds a critical value (which depends on the filling ν , i.e. on the Luttinger interaction constant). This is a pure non-equilibrium effect, since the maximum occurs only at finite driving $V \neq 0$. Of course, the total current still *decreases* as the point-contact interaction strength is increased. This feature is consistent with the first-order perturbative results [5] for the $I(V)$ curves at zero temperature, in the strong and weak backscattering limits.

When there is a single relevant operator corresponding to the impurity, the model is integrable, so we compute the current and conductance exactly. There is only one relevant operator when $\nu = 1/3$, so integrability is generically observed without any fine tuning. Any other sample-specific details appear only in the irrelevant operators. Integrability allows the definition of a basis of massless charge-carrying ‘quasiparticle’ excitations [8,9]. These quasiparticles are scattered one-by-one off the impurity with a momentum-dependent one-particle scattering matrix S of transmission and reflection amplitudes. These amplitudes can be determined exactly by imposing the constraints of integrability, including the boundary Yang-Baxter equation and the boundary-crossing relation [8]. Furthermore, the quasiparticles are characterized by an thermal distribution function which can be calculated exactly using the thermodynamic Bethe ansatz [10,11]. This special behavior is a consequence of integrability, and it allows us to derive an exact rate (Boltzmann) equation for the conductance in this interacting theory.

We should note that many of these results have been checked by using a completely different method of computation. Instead of the non-perturbative methods to be described below, one can study the model perturbatively in the interaction strength T_B . Closed-form results for all the perturbative coefficients of the free energy have been found; a simple technical assumption then also leads to closed-form expressions for all the perturbative coefficients of the conductance, even at finite V [12]. There is complete qualitative and quantitative agreement between the two approaches.

The outline of this paper is as follows: In sect. 2 we discuss how this system is realized in experiments on resonant tunneling through point contacts in fractional quantum Hall devices. In sect. 3, we map the problem into two decoupled theories, one of which is affected by the backscattering interaction, and another one which is not. In sect. 4 we find the exact quasiparticle spectrum, exact S matrices for quasiparticles scattering among

themselves and off of the boundary, and the exact thermal distribution functions, using the fact that the interacting theory is integrable. In sect. 5, we derive an exact (Boltzmann) equation for the current in terms of the S matrix and the distribution functions. This gives us equations for the exact conductance. These can easily be solved numerically, and we present curves for a variety of values. At zero temperature, the equations simplify and we present more explicit analytic results in sect. 6. This enables us to derive an exact duality between strong and weak backscattering limits, out of equilibrium.

2. The fractional quantum Hall effect

2.1. *Experimental setting for resonant tunneling*

Experiments on resonant tunneling between two $\nu = 1/3$ edges have recently been performed by Milliken, Umbach and Webb [2]. We briefly review the experimental setup schematically (for details see [2,6]). A fractional quantum Hall state with filling fraction $\nu = 1/3$ is prepared in the bulk of a quantum Hall bar (discussed in Section 1). This means that the bulk quantum Hall state is prepared in a Hall insulator state (longitudinal conductivity $\sigma_{xx} = 0$), and that the (bulk) Hall resistivity is on the $\nu = 1/3$ plateau where $\sigma_{xy} = (1/3)e^2/h$. This is achieved by adjusting the applied magnetic field, perpendicular to the plane of the bar. Since the plateau is broad, the applied magnetic field can be varied over a significant range without affecting the filling of $\nu = 1/3$. Next, a gate voltage V_g is applied perpendicular to the long side of the bar, i.e. in the y direction (see Section 1) at $x = 0$. This has the effect of bringing the right and left moving edges close to each other near $x = 0$, forming a point contact. Away from the contact there is no backscattering (i.e. no tunneling of charge carriers) because the edges are widely separated, but now charge carriers can hop from one edge to the other at the point contact.

The linear-response source-drain conductance as a function of temperature and gate voltage V_g has been measured experimentally [2]. As the gate voltage is swept through, the conductance signal shows a number of resonance peaks, which sharpen as the temperature is lowered. These resonance peaks occur for particular values $V_g = V_g^*$ of the gate voltage, due to tunneling through localized states in the vicinity of the point contact. Ideally, on resonance, the source-drain conductance is equal to the Hall conductance without point contact, i.e. $G_{resonance} = (1/3)e^2/h$. This value is independent of temperature, on resonance. Now, measuring the linear response conductance as a function of the gate voltage

near the resonance, i.e. as a function of $\delta V_g \equiv V_g - V_g^*$, at a number of different temperatures T , one gets resonance curves, one for each temperature. These peak at $\delta V_g = 0$. Scaling arguments imply [5] that those experimental conductance curves should collapse onto a single universal curve when plotted as a function of $\delta V_g/T^{2/3}$. Indeed they do collapse quite well [2]. Moreover, the resulting universal curve should be a unique signature and fingerprint of the $\nu = 1/3$ edge state in the leads connected to the point contact.

2.2. *Comparison of the linear response resonance lineshape with our exact Luttinger model predictions*

To make contact with the Luttinger model, we state (as will be explained below in more detail) that the experimental parameter δV_g should be related to the Luttinger backscattering interaction by $\delta V_g \propto T_B^{2/3}$. In particular, at the resonance value $T_B = 0$, there is no backscattering at all.

We have compared [1] our exact predictions for the linear response conductance scaling curve with the experimental data [2] as well as Monte Carlo calculations in [6]. The agreement between the Monte Carlo simulation and our exact scaling curve is excellent. The exact value of the universal parameter K (defined so that $G(X) = KX^{-6}$ for X large and $G(X) = (1 - X^2)/3$ for X small) is $K = 3.3546\dots$ (where $X \approx .74313(T_B/T)^{2/3}$). (The value $K \approx 2.6$ quoted in [6] seems to have been slightly underestimated there.)

The comparison with the existing experiments by Milliken et al is not completely straightforward, since the conductance at the resonance peak in the experimental data decreases with temperature and is well below its resonance value $e^2/3h$. This difficulty arises since in order to achieve the resonance condition in the Luttinger model, two parameters need to be tuned, since the point contact will in general not possess reflection-parity symmetry about the point $x = 0$ [13]. In the experiments performed so far only one parameter, namely V_g , has been tuned. For that reason, the conductance peaks do not have their maximum height $G_{resonance} = (1/3)e^2/h$, but are smaller, and, furthermore, the peak height does decrease with temperature, reflecting the fact that the experimental peak is not a perfect resonance. This problem can be remedied in a future experiment, by varying *two* parameters, namely V_g and the magnetic field on the plateau, instead of only one parameter, to achieve resonance. Nevertheless, even when only the gate voltage is tuned to resonance, the experimental data for the conductance signal as a function of the gate voltage and temperature collapse well onto single scaling curve. Thus it makes sense to compare the this experimental curve with our exact conductance curve, computed

from the Luttinger model. The agreement is quite good, given the large scatter of the data in the tail of the resonance curve. In particular, the data clearly show the predicted $G \propto T^4/(V_g - V_g^*)^6$ behavior in the tail.

2.3. Predictions for future non-equilibrium transport measurements

In principle, there is no reason why the above mentioned measurements could not be extended to finite driving voltage V [one should not confuse the driving voltage V , which is the difference between the chemical potentials between the injected left- and right-moving charge carriers, with the gate voltage V_g , which gives rise to the coupling constant T_B in the Luttinger liquid theory]. So far, only the linear-response conductance, $G = \lim_{V \rightarrow 0} I(V)/V$ has been measured. More generally, one could attempt to measure the conductance at *finite* driving voltage V . Note that our exact results predict the shape of the universal scaling function

$$G(T_B/T, V/T), \quad T_B = C(\delta V_g)^{3/2}$$

as a function of *two* ratios. The non-universal parameter C is determined by fitting the experimental data to the universal curve; this is the only unknown quantity. The linear-response conductance is the limit of this function as $V \rightarrow 0$, where it becomes a function only of one ratio T_B/T . Note that the conductance at finite driving voltage V also describes a resonance lineshape. A particularly interesting feature of the conductance at finite driving voltage V is seen in fig. 1. The conductance as a function of $T_B \propto (\delta V_g)^{3/2}$ develops a pronounced peak when the ratio of driving voltage to temperature $eV/k_B T$ exceeds a critical value 7.188.... For a typical low temperature $T = 50mK$ used in the data of [2], this would correspond ($10k_B K = 1meV$, or, $\frac{5\mu V}{50mK} = 1$) to a driving voltage of $V^* \approx 35\mu V$. The current data were taken at an ‘excitation voltage’ of $1\mu V$, which corresponds to a ratio $eV/k_B T \approx 0.2$. We have plotted the exact results for the aforementioned scaling functions in Figs. 1 and 2. One sees clearly from these plots that $eV/k_B T \approx 0.2$ corresponds to the linear response regime. Perhaps the most significant feature displayed in Fig. 2 is a very dramatic *non-equilibrium broadening* of the resonance curve for values of the ratio V/T even well below the occurrence of the maximum. In terms of numbers, the curve broadens by a dramatic amount already at $eV/k_B T \approx 2$ or 3, well before the onset of the maximum (at $eV/k_B T \approx 7.188$). This broadening should be easily visible experimentally, since it would correspond to an excitation voltage $V \approx 15\mu V$, just a factor of 15 higher than the ones used by Milliken et al., at $T = 50mK$.

Clearly, at larger voltages one will have to worry about larger currents flowing in the sample, which might lead to possible complications. These complications would for example include non-universal effects arising from sample heating which are clearly not included in the Luttinger theory and which could mask the underlying universal Luttinger non-fermi liquid physics. However one should notice that for most part of the conductance curve the conductance is very small, implying flow of very small currents, so that sample heating should not appear to be a problem.

Futhermore, it is important to notice that the scaling function depends only on the ratio V/T . This means the same critical ratio $(V/T)^* = 7.188$ could also be achieved by working at lower temperatures. It might be reasonable experimentally to perform measurements at lower temperatures. This would reduce even more the values of the driving voltage where the onset of the universal non-equilibrium features (the most dramatic one being the broadening) become clearly visible.

3. Bosonizing and mapping to an integrable model

The Luttinger model is the most general model of a single massless fermion in one dimension. The fermion interaction is governed by a single parameter g_{Lutt} , so that when $g_{Lutt} > 0$ the interaction is repulsive and $g_{Lutt} < 0$ it is attractive. In the absence of the impurity, the Hamiltonian is

$$H = \pi \int_{-l}^l dx (J_L^2 + J_R^2 + g_{Lutt} J_L J_R) \quad (3.1)$$

where the left movers are coupled to the right. We use the well-known map of this model to free massless left and right moving bosons Φ_L and Φ_R [14]. To do so one bosonizes the currents $J_L = -\frac{1}{2\pi} \partial_x \Phi_L$ and $J_R = \frac{1}{2\pi} \partial_x \Phi_R$. The fermion operators take also the form $\Psi_R =: e^{i\Phi_R} :$ and $\Psi_L =: e^{i\Phi_L} :$. By introducing new fields [15] using the transformation (canonical up to a global factor $\sqrt{\alpha}$)

$$\begin{aligned} \Phi_R &= \frac{\alpha+1}{2} \varphi_R + \frac{\alpha-1}{2} \varphi_L \\ \Phi_L &= \frac{\alpha-1}{2} \varphi_R + \frac{\alpha+1}{2} \varphi_L, \end{aligned} \quad (3.2)$$

one can decouple the interaction in the bosonized hamiltonian that reads then

$$H_0 = \frac{\pi}{\nu} \int_{-l}^l dx [j_L^2 + j_R^2] = \frac{1}{8\pi\nu} \int_{-l}^l \Pi^2 + (\partial_x \varphi)^2, \quad (3.3)$$

where Π is canonical momentum conjugate to ϕ . The coefficient ν is related to the old Luttinger coupling via $g_{Lutt} = -2\frac{\alpha^2-1}{\alpha^2+1}$, $\frac{1}{\nu} = \frac{2\alpha^2}{1+\alpha^2}$. The currents $j_L = -\frac{1}{2\pi}\partial_x\varphi_L$ and $j_R = \frac{1}{2\pi}\partial_x\varphi_R$ are then normalized so that $\langle j_L(x_1)j_L(x_2) \rangle = \frac{\nu}{(2\pi)^2(x_1-x_2)^2}$ which makes the meaning of ν as a chiral $U(1)$ anomaly explicit. The operators $\psi_R =: e^{(i/\nu)\varphi_R}$: and $\psi_L =: e^{(i/\nu)\varphi_L}$: are sometimes referred to as “Luttinger hyperfermion” operators when $1/\nu$ is an odd integer [16]. There are two $U(1)$ symmetries of this model corresponding to left and right (hyper) fermion number: we introduce the corresponding conserved charges $Q_L = \int_{-l}^l dx j_L$, and $Q_R = \int_{-l}^l dx j_R$. The corresponding “hyperfermions” have charge e as do the original electrons, as can be seen by computing their commutators with the charge operators.

We now include an impurity, which we assume is localized at the origin $x = 0$. It couples left- and right-moving fermions with the interaction $\Psi_L^\dagger(0)\Psi_R(0) + \Psi_R^\dagger(0)\Psi_L(0)$. Such a coupling destroys the separate conservation of the two charges Q_L and Q_R : only the *total* charge $Q_L + Q_R$ remains conserved, corresponding to simultaneous phase translations of φ_L and φ_R . In a renormalized effective theory, all terms that are not forbidden by total charge conservation symmetry can appear in the hamiltonian. These may be represented in terms of the bosons φ_L, φ_R by a backscattering contribution to the Hamiltonian [4,5] :

$$H_B = \frac{1}{2} \sum_n \lambda_n \{ e^{in\varphi_L(x=0)} e^{-in\varphi_R(x=0)} + e^{-in\varphi_L(x=0)} e^{in\varphi_R(x=0)} \}. \quad (3.4)$$

When we describe the Luttinger theory in terms of the bosons φ_L and φ_R , i.e. after the Luttinger bulk interaction g_{Lutt} has been disentangled, this term describes hopping of quasiparticles of charge νe (the Laughlin quasiparticles in the case of FQHE) between the left- and right-moving edges. Only the terms with $n^2 < 1/\nu$ are relevant. For $\nu > 1$ all terms are irrelevant; this case is more appropriately described by a “dual” picture [5]. At $\nu = 1$ there is a single exactly marginal operator. This preserves the conformal invariance of the fixed point, so conformal techniques are applicable, making possible the calculation of the complete partition function [17]. We now focus on the case $\nu < 1$. For the model to be integrable, it seems that only one relevant perturbation is allowed [8]. Thus when $1 > \nu > 1/4$, the backscattering interaction is *automatically* integrable without *any* fine-tuning. The experimentally-measured value of $\nu = 1/3$ falls into this range of parameters. For $\nu < 1/4$, the model has to be fine-tuned in order to be integrable. In particular, for $1/9 < \nu < 1/4$ a single parameter (λ_2) needs to be tuned to zero in order to achieve integrability. In general, we will be treating the model with $\lambda_n = 0$ for $n \geq 2$.

In order to transport net charge through the impurity, we place the injected left movers and the right movers at different chemical potentials. This amounts to adding a term $e(Q_L - Q_R)V/2$ to the Hamiltonian describing the thermal weighting of the injected charge carriers. Notice that even though this problem is out of equilibrium for non-zero V , the charge carriers injected into the leads are thermally weighted with an equilibrium distribution function corresponding to μ_L or μ_R . Thus we are studying the coupling between two equilibrium distributions.

It is convenient to introduce the “backscattering temperature” T_B , which is the scale generated by the relevant point contact coupling constant at one point:

$$T_B = C_1 \lambda_1^{1/(1-\nu)}$$

where C_1 is some non-universal constant. When there is no backscattering, $T_B = 0$. The exponent follows from a simple perturbative analysis [5]. For $\nu < 1/2$ and $T > 0$ there are actually no divergences in the coefficients of the perturbative expansion; we exploit this fact in Sect. 6 to derive C_1 exactly. The conductance G and current I are universal scaling functions of two dimensionless ratios, for example T_B/T and V/T . Since T_B is a scale introduced by the (local) impurity, a bulk quantity like the leading part of the thermal distribution functions is independent of the point contact interaction and can be computed without the point contact. In other words, the corrections vanish with the size of the system.

We now map the model including the impurity to an integrable model. By taking (non-local) linear combinations of the bosons, we can first map the left- and right-moving bosons to a purely left-moving system. Calling these left movers *even* and *odd*, we have

$$\begin{aligned}\phi^e(x+t) &\equiv \frac{1}{\sqrt{2}}[\varphi_L(x,t) + \varphi_R(-x,t)], \\ \phi^o(x+t) &\equiv \frac{1}{\sqrt{2}}[\varphi_L(x,t) - \varphi_R(-x,t)]\end{aligned}\tag{3.5}$$

where these particles are defined on $-l < x < l$. One replaces j_L, j_R with j^e, j^o in the Hamiltonian (3.3), where $j^{e/o}(x+t) = (1/\sqrt{2})[j_L(x,t) \pm j_R(-x,t)]$ are the charge densities of even and odd bosons. For purposes of computing the backscattering current, the non-locality of this transformation does not matter (it clearly would if we were to compute spatially-dependent Greens functions). Two major simplifications arise from this change of basis. First, the interaction involves only the combination $\varphi_L(x=0) - \varphi_R(x=0)$ so

only the odd boson ϕ^o interacts, while the even boson ϕ^e remains free [18]. (This was the crucial step in solving the X-ray edge problem in a Luttinger liquid [19].) Second, the backscattering current I_B can be entirely expressed in terms of the odd boson theory. This is easy to see: The even and odd charges are related to the charges of the original left- and right-moving edges by $\Delta Q = Q_L - Q_R = \sqrt{2}Q^o$ and $Q_L + Q_R = \sqrt{2}Q^e$. Thus Q^e measures the total charge on both edges and is conserved even in the presence of the interaction. Therefore, the even boson decouples from the quantities we study (although it does enter into the determination of the spectrum at the fixed points [18]) and will play no role in the following. Moreover, the backscattering current is the rate at which the charge difference between right and left edges decreases (see below). It is thus directly related to the odd charge by $\partial_t \Delta Q$.

The constraint of integrability is a very powerful one. As we will see, it enables the calculation of exact thermal distribution functions in an interacting theory. Not surprisingly, only certain models are integrable. The impurity is also significant; only particular types of impurity couplings preserve the integrability. The Luttinger model without the impurity is well known to be integrable, but it is easily shown that before the non-local map (3.5), the impurity destroys the integrability. However it *is* integrable in the odd-boson basis. The integrability of the impurity interaction in the Luttinger model was first established by [8] in the context of the boundary sine-Gordon model. In order to make contact with this work, we map our theory involving the *massless* left-moving odd boson ϕ^o on the line, with the point contact interaction at the origin $x = 0$, into a boundary sine-Gordon problem. This is done using a standard “folding” procedure. From the left-moving odd boson $\phi^o(x + t)$ on the full line, we define right *and* left moving odd bosons on the half line $x > 0$ by

$$\begin{aligned}\phi_L^o(x, t) &\equiv \phi^o(x + t), & x > 0 \\ \phi_R^o(x, t) &\equiv \phi^o(-x + t), & x > 0\end{aligned}$$

This model is no longer chiral, but lives on the half-line.

There are many field theories on the half-line which are integrable, the Kondo model being a celebrated example [20]. Recently much effort has gone into understanding their properties. In the following we exploit the results of [8]. The odd-boson model with interaction becomes the massless limit $\Lambda \rightarrow 0$ of the massive sine-Gordon model on the half-line

$$H_{SG} = \frac{1}{8\pi\nu} \int_0^l dx \left[(\partial_x \phi^o)^2 + (\Pi^o)^2 + \Lambda \cos \sqrt{2}\phi^o \right] + \lambda_1 \cos \frac{1}{\sqrt{2}}\phi^o(0) \quad (3.6)$$

[Π^o is the canonical momentum conjugate to the odd-boson field ϕ^o .] This model is integrable for any value of the bulk mass Λ , and the Luttinger parameter ν [8]. However, the factor of two ratio in the argument of the bulk and boundary cosines seems to be necessary for the integrability. In the standard sine-Gordon conventions where the first term has a $1/2$ in front, our normalization corresponds to $\beta_{SG}^2 = 8\pi\nu$. A lattice regularization of this field theory, the XXZ spin chain with a σ_x perturbation on the boundary, was long ago shown to be integrable [21].

Notice that we can “fermionize” to get back a Luttinger model (for $\Lambda \neq 0$ we get the massive Thirring model) on the half-line for the odd-boson degree of freedom. However, because of the non-linear change of basis in (3.5), the properties of the odd-boson Luttinger model are not the same as the original model. In particular, the original Luttinger model is a free fermion when $\nu = 1$, while the odd-Luttinger fermion is free when $\nu = 1/2$. This shift arises because of the $\sqrt{2}$ in (3.5), which is necessary to keep the same normalization of the kinetic term. Thus an interacting fermion on the full line can be mapped to a non-interacting one on the half-line. This provides a simple way of understanding the results of [22], where the $\nu = 1/2$ model is mapped onto two Ising models, one of which has a boundary magnetic field. Two Ising models are well known to be equivalent to a free Dirac fermion (up to boundary conditions), and it is easily seen that H_B corresponds to a boundary magnetic field on one of them.

To recover our massless model, we simply have to take the $\Lambda \rightarrow 0$ limit [9]. So we see that, after the few mappings described above, our impurity problem is integrable as long as only one of the impurity coupling constants λ_n in (3.4) is non-zero. As noted before, this is natural for $1 > \nu > 1/4$, where power counting shows that only the first coupling constant λ_1 is relevant.

4. The quasiparticles, their S matrix and their distribution functions

4.1. The quasiparticle spectrum

We find the appropriate quasiparticle basis by studying the model (3.6) at arbitrary Λ . As discussed carefully in [9], the quasiparticle spectrum remains the same in the massless limit $\Lambda \rightarrow 0$ of the massive sine-Gordon model on the half-line (3.6). Introducing the parameter Λ and then setting it to zero is not necessary for solving the problem, but it gives an easy way of finding the basis where the quasiparticles scatter off the boundary without particle production.

Integrability means that there is an infinite number of conserved quantities which commute with each other and with the Hamiltonian, even in the presence of the impurity (3.4) [8]. From this we see already that in an integrable system a particular basis of Hilbert space, in which all the infinite conserved quantities as well as the hamiltonian are *diagonal*, plays a special and simplifying role. It is this basis on which we will focus. This basis has a “quasiparticle” structure similar to the “particle” Fock space of a non-interacting theory. In particular, the eigenvalues of the infinite conserved quantities in this basis have the form $\sum_i p_i^n$, where p_i are momenta of individual quasiparticles, and where n runs over an infinite subset of the positive integers (each n labels one conservation law). In the Luttinger model these run over n odd. The identification of p_i as momenta of “quasiparticles” arises from the form of the eigenvalue of the Hamiltonian in this basis, which is $H = v_F \sum_i p_i$. This means that the energies of the “quasiparticles” are additive, justifying the association of the particle concept with those eigenstates.

These conservation laws have important consequences for scattering. The quasiparticles of this basis must scatter off the impurity *without* particle production, i.e. one-by-one. This means that the scattering matrix off the point contact is a product of 1-body S matrices, one for each quasiparticle. Away from the impurity (in the “bulk”), the quasiparticles scatter off of each other with a completely elastic and factorizable two-body scattering matrix S^{bulk} . This follows from an old kinematic argument [23,24] which applies when there is any conservation law with $n > 1$. Factorizability means in the bulk that the N -body bulk S matrix is a product of 2-body S matrices S^{bulk} . Completely elastic means that *individual* momenta are conserved in a collision: all that can happen is that the momenta of the particles get permuted. This does not mean that bulk scattering is trivial; internal quantum numbers can change, and even if scattering is diagonal (i.e. internal quantum numbers do not change), the particles can have a phase delay, i.e. the S matrix may be a momentum-dependent phase.

There are many bases for the Hilbert space of the *massless* odd-boson theory, which are related by not-necessarily-local mappings. For example, plane waves obviously are eigenstates of H_0 , but they are not eigenstates of $H_0 + H_B$ [9]. The basis of particles of (3.6) which are eigenstates has been known for some time [24]. (Indeed, in a massive theory there is only one particle basis; it is only for $\Lambda = 0$ in (3.6) that there is a choice.) At any value of ν , the spectrum contains a kink (+) and an antikink (−). These carry (odd) charges $Q^o = 1/\sqrt{2}$ and $-1/\sqrt{2}$, respectively. Moreover, for $n - 1 < 1/\nu \leq n$, there are $n - 2$ “breather” states which have no charge. These breathers exist in the regime

where the fermion interaction in the odd-Luttinger model is attractive; in this language they correspond to fermion-antifermion bound states. These particles span the Hilbert space of the left-moving odd boson; we label them by indices j, k, \dots running over the kink (+), antikink (−) and breathers (b). One can in fact check explicitly that these particles are the solutions of the classical limit of (3.6) for any value of Λ [9].

Henceforth, we set $\Lambda = 0$ in (3.6) so that the particles are massless. We also ignore the even boson, since it does not affect the current or conductance. We will find more convenient to use the unfolded language, so we will continue to discuss a purely left-moving theory on the full line with an impurity.

Since the particles are massless, a left mover has dispersion relation $E = -p$. Instead of momentum, we use rapidity θ , which for a particle of type j is defined as

$$E = -p = m_j e^\theta,$$

where $m_k = M \sin(k\pi\nu/2(1 - \nu))$ for the k th breather and $m_\pm = M/2$. The overall scale M is arbitrary and cancels out of all physical results.

Notice that the momenta of the quasiparticles all have one sign (the rapidity θ is real). Since this might be unfamiliar, we now express the charged fermions occurring for $\nu = 1/2$ in terms of kink and antikink quasiparticles; for $\nu = 1/2$ there is no breather. Recall that for $\nu = 1/2$ we can re-fermionize the odd-boson theory. Thus we obtain a single non-interacting, spinless charge fermion $\psi^\dagger(p), \psi(p)$ where the momentum p runs over all real values (positive and negative). This fermion satisfies canonical anticommutation relations, since it is non-interacting. The kinks and antikinks for this simple theory can be defined using a canonical particle-hole transformation:

$$\begin{aligned}\psi_+(p) &\equiv \psi(p) && (kink) \\ \psi_-(p) &\equiv \psi^\dagger(-p) && (antikink)\end{aligned}$$

for $p > 0$. The left-hand-side defines kink and antikink annihilation operators. Similarly, the kink and antikink creation operators are the hermitian conjugates:

$$\begin{aligned}\psi_+^\dagger(p) &\equiv \psi^\dagger(p) && (kink) \\ \psi_-^\dagger(p) &\equiv \psi(-p) && (antikink)\end{aligned}$$

for $p > 0$. Thus for $\nu = 1/2$ kinks and antikinks are just particle-hole transforms of ordinary fermions, and have only one sign of momentum. Unfortunately, for $\nu \neq 1/2$ the mapping is not as straightforward.

While there are no statistics in $1 + 1$ dimensions (there is no way to bring a particle around another without interacting), a crucial issue is how many particles are allowed to occupy each level. The answer is well established in the massive sine-Gordon model: only one quasiparticle is allowed per level (they are like fermions). This is basically because the Bethe-ansatz wave function used to solve the model or its regularized lattice versions vanishes when two or more excitations have the same rapidity. It is possible to study similarly a regularized lattice version of the massless limit of the sine-Gordon model [25,26] and to see that the same exclusion principle holds in that limit. This does not contradict other ways of describing the excitations, where the particles are free but obey “exclusion statistics” [27]. These particles seem to be related to the quasiparticles of the Calogero-Sutherland model, or the Haldane-Shastry spin chain. In the realization of the Luttinger liquid in the fractional quantum Hall effect discussed in sect. 2, these particles are the Laughlin quasiparticles restricted to the edge. These particles are clearly not the same as ours; for example they are the quasiparticles of the original Luttinger impurity problem, while ours are those of the odd boson theory, which is found from the original by a non-local map. This means that there are (at least) two sets of bases of quasiparticles for the Luttinger liquid, one where the particles are free but fill levels in a peculiar manner, and another, where the particles fill levels like fermions but interact. In the first approach, however, it is not known yet how to include an impurity. If this problem is solved, it would be very interesting to compare the two methods of calculation.

4.2. The bulk and impurity S matrices

These massless kinks and breathers interact with each other and with the impurity. Even though the model away from the impurity is a free boson, an effect of using this quasiparticle basis is that the particles interact even in the bulk. We describe these interactions with bulk and impurity scattering matrices. First, we have an S matrix for a particle scattering off of the impurity. Since the integrability requires that the particles scatter one-by-one, this can be described by one-particle S matrix elements. Kinematically, all that happens is the particle goes through the impurity with a phase delay. Because the impurity interaction violates odd-charge conjugation, it is possible for the positively-charged kink to scatter into a negatively-charged antikink when going through the impurity.

Dimensional analysis tells us that the S matrix elements must depend only on the ratio p/T_B . If we define the “backscattering rapidity” by the relation

$$T_B = \frac{M}{2} e^{\theta_B},$$

this means that all impurity S matrix elements depend on the rapidity difference $\theta - \theta_B$. Thus the impurity-kink S matrix consists of the elements $S_{++}(\theta - \theta_B) = S_{--}(\theta - \theta_B)$ for kink \rightarrow kink, and antikink \rightarrow antikink, as well as $S_{+-}(\theta - \theta_B) = S_{-+}(\theta - \theta_B)$ for kink \rightarrow antikink, and vice versa. These S matrix elements are given by taking the massless limit of the results of [8]:

$$\begin{aligned} S_{++}(\theta) &= \frac{\exp(\lambda\theta)}{1 + i \exp(\lambda\theta)} \exp[i\alpha_\nu(\theta)] \\ S_{+-}(\theta) &= \frac{1}{1 + i \exp(\lambda\theta)} \exp[i\alpha_\nu(\theta)]. \end{aligned} \tag{4.1}$$

Here $\exp[i\alpha_\nu]$ is the phase of the expression given in Eq.(3.5) of [9]. For convenience we have defined

$$\lambda \equiv \frac{1}{\nu} - 1.$$

The boundary S matrix is unitary: $|S_{++}|^2 + |S_{+-}|^2 = 1$. The S matrix is such that for particle with very large energy (UV limit), the scattering is diagonal. Diagonal scattering in the unfolded theory is totally off-diagonal scattering in the folded one, so matrix elements here are interchanged as compared to [9].

Because we are no longer working in the plane-wave basis, it is also necessary to find the non-trivial S matrix for particles interacting in the bulk. Since all particles are massless, they must all have the same velocity v_F (which is set to 1 in this paper). Thus it is not immediately obvious how to define an S matrix for two left movers. It is best interpreted as a matching condition on the Bethe wave function, as we will explain in the next subsection. Alternatively, one can think of acting on multiparticle states with creation and annihilation operators: the non-trivial S matrix means that these operators satisfy non-trivial commutation relations, the so-called Zamolodchikov-Faddeev algebra [24]. Since there is no mass scale in the bulk (only T_B at the impurity), a two-particle bulk S matrix element can only depend on the ratio of the two momenta p_1/p_2 . In terms of rapidity, this is a function of $\theta_1 - \theta_2$. Thus we can now think of the impurity as a particle with rapidity θ_B and a different S matrix than the bulk one.

For general ν , the left-left two-particle S matrix is given by the same formula as in the massive case. This S matrix is not diagonal: the initial state $|K(\theta_1)A(\theta_2)\rangle$ can scatter to $|A(\theta_1)K(\theta_2)\rangle$ because the kink K and antikink A have the same mass. For the kink/antikink scattering one has three amplitudes [24]

$$\begin{aligned} a(\theta) &= \sin[\lambda(\pi + i\theta)]Z(\theta) \\ b(\theta) &= -\sin(i\lambda\theta)Z(\theta) \\ c(\theta) &= \sin(\lambda\pi)Z(\theta). \end{aligned} \tag{4.2}$$

where the S matrix element $a(\theta_1 - \theta_2)$ describes the process $|K(\theta_1)K(\theta_2)\rangle \rightarrow |K(\theta_1)K(\theta_2)\rangle$, as well as $|A(\theta_1)A(\theta_2)\rangle \rightarrow |A(\theta_1)A(\theta_2)\rangle$, b describes $KA \rightarrow KA$, c describes the non-diagonal process $KA \rightarrow AK$, and there is a symmetry under interchange of kink to antikink (corresponding to $\phi^o \rightarrow -\phi^o$). The function $Z(\theta)$ is a normalization factor, which can be written as

$$Z(\theta) = \frac{1}{\sin[\lambda(\pi + i\theta)]} \exp \left(i \int_{-\infty}^{\infty} \frac{dy}{2y} \sin \frac{2\theta\lambda y}{\pi} \frac{\sinh[(\lambda - 1)y]}{\sinh y \cosh[\lambda y]} \right).$$

The breather-kink and breather-breather S matrices are well known [24]; we do not write them down here.

When $1/\nu$ is an integer, the bulk scattering is diagonal (c vanishes) and $a = \pm b$. Therefore, the only allowed processes are of the form $|j(\theta_1)\rangle \otimes |k(\theta_2)\rangle \rightarrow |k(\theta_2)\rangle \otimes |j(\theta_1)\rangle$. Such a process is described by the S matrix element $S_{jk}^{bulk}(\theta_1 - \theta_2)$. However, the impurity scattering is not diagonal, so charge transport is still possible. The bulk diagonal scattering makes the thermodynamic Bethe ansatz computation discussed in the next subsection much simpler at these values of ν .

4.3. The non-fermi distribution functions

As with the S matrix, it is convenient to use rapidity instead of momentum or energy to define the densities of states and distribution functions. The number of allowed kink or antikink states per unit length with rapidity between θ and $\theta + d\theta$ is given by $n_{\pm}(\theta, V)d\theta$, while the number of states actually occupied by kinks or antikinks in this rapidity range is $n_{+}(\theta, V)f_{+}(\theta, V)d\theta$ and $n_{-}(\theta, V)f_{-}(\theta, V)d\theta$, respectively. Thus

$$\langle \Delta Q \rangle_V = 2l \int_{-\infty}^{\infty} d\theta [n_{+}(\theta, V) f_{+}(\theta, V) - n_{-}(\theta, V) f_{-}(\theta, V)]. \quad (4.3)$$

Since at most one kink is allowed per level, we have $0 \leq f_{\pm} \leq 1$. The functions n_j and f_j are defined for the breathers in the same manner.

These thermodynamic functions $n_j(\theta)$ and $f_{\pm}(\theta, V)$ are different from the free-fermion functions when the odd-boson kink theory is an interacting Luttinger liquid ($\nu \neq 1/2$), but we can derive them exactly. The idea is simple, and has become known as the thermodynamic Bethe ansatz [11]. It is basically the same as what is used in exact solutions of other impurity problems like the Kondo problem [20]. The main difference between the approach used here and the traditional approach is that in the latter, the Bethe ansatz appears as

a tool to diagonalize a bare hamiltonian, while here we work directly in the renormalized theory where factorized scattering is assumed, and the Bethe-ansatz equations (here relations between n and f) follow simply from a matching condition on the Bethe wave function. This matching condition gives one set of equations relating the functions n_j and f_j . Following the standard thermal approach to Bethe ansatz [10], one writes the free energy as a functional of n and f and minimizes it. Together with the first equation from the matching condition, this second set of equations from the minimization requirement yields n and f .

The simplest situation occurs when the scattering is completely diagonal, which occurs when $1/\nu$ is an integer. Here we can easily impose periodicity of the Bethe wave function since we know the S matrix, which encodes the change of the wave function when two particles (or a particle and the impurity) are interchanged. Thus we know the phase the wave function picks up when a particle is brought “around the world” through all the others. We denote generically the kink, antikink and breathers by the index j , so the two-particle S matrix elements are labeled by $S_{jk}(\theta_1 - \theta_2)$. In the following calculation of the densities n and f , we can ignore the phase shift due to scattering on the impurity because it affects densities only to order $1/l$, where l is the system size. This does not affect the densities in the thermodynamic limit $l \rightarrow \infty$, and will therefore not show up in the computation of the conductance. (On the other hand, however, in the absence of the voltage these $1/l$ effects on the densities can be computed and are responsible for the impurity free energy [9].) The requirement of a periodic boundary condition under this operation quantizes the momenta:

$$e^{-im_{r_i} \exp(\theta_i)l/\hbar} \prod_{j=1, j \neq i}^{\mathcal{N}} S_{r_i r_j}(\theta_i - \theta_j) = 1, \quad (4.4)$$

where $E = -P = m_j \exp(\theta)$ for a particle of type j . The periodicity condition (4.4) includes the interaction of any particle with all the others. By taking a derivative with respect to the rapidity of the logarithm of (4.4), one finds

$$n_j(\theta) = \frac{m_j e^\theta}{h} + \sum_k \int_{-\infty}^{\infty} d\theta' \Phi_{jk}(\theta - \theta') n_k(\theta') f_k(\theta'), \quad (4.5)$$

where $\Phi_{jk}(\theta) = -i(d/d\theta) \ln S_{jk}^{bulk}(\theta)/2\pi$ [10]. For example, for $\nu = 1/3$ there is one breather (b) and [28]

$$\begin{aligned} \Phi_{bb}(\theta) &= 2\Phi_{++}(\theta) = 2\Phi_{+-}(\theta) = -\frac{1}{\pi \cosh \theta} \\ \Phi_{b+}(\theta) &= \Phi_{+b}(\theta) = -\frac{\sqrt{2} \cosh \theta}{\pi \cosh 2\theta}, \end{aligned} \quad (4.6)$$

while the others follow from the symmetry $+\leftrightarrow -$. Explicit expressions for $\Phi_{jk}(\theta)$ in the more general case where $1/\nu$ is a positive integer are given in Eq.(4.9) of [9], and in [28].

One defines an auxiliary pseudoenergy variable ϵ_j to parametrize f_j via

$$f_j \equiv \frac{1}{1 + e^{-\mu_j/T} e^{\epsilon_j}},$$

where the μ_j are the chemical potentials: $\mu_+ = -\mu_- = eV/2$; $\mu_b = 0$. By demanding that the free energy at temperature T (expressible in terms of f_j and n_j) be minimized, we find an equation for ϵ_j in terms of the (known) bulk S matrix elements:

$$\epsilon_j(\theta, V/T) = \frac{m_j e^\theta}{T} - \sum_k \int_{-\infty}^{\infty} d\theta' \Phi_{jk}(\theta - \theta') \ln[1 + e^{\mu_k/T} e^{-\epsilon_k(\theta, V/T)}]. \quad (4.7)$$

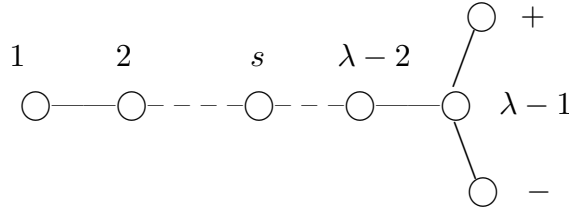
Solving this system of coupled integral equations for ϵ_j gives the functions f_j . Except in special cases, this solution cannot be obtained in closed form, but it is easy to solve these equations numerically. We will not need the explicit Φ_{jk} , because the equations (4.7) can be simplified by using an trigonometric identity described in [29,30] for example. Denoting convolution by \star

$$f \star g(\theta) \equiv \int d\theta' f(\theta - \theta') g(\theta')$$

one finds

$$\Phi_{jk}(\theta) = \sum_l N_{kl} K \star (\Phi_{jl}(\theta) + \delta_{jl} \delta(\theta)) \quad (4.8)$$

where the kernel $K(\theta) \equiv \lambda/(2\pi \cosh \lambda\theta)$, and N_{jk} is the incidence matrix of the following diagram



i.e. $N_{jk}=1$ if the nodes j and k are connected, and 0 otherwise (in particular $N_{jj} = 0$). This identity follows simply by Fourier transforming the Φ_{jk} and using trigonometric identities. We show this explicitly for $\nu = 1/3$ ($\lambda = 2$) in Appendix B. Thus the simplified form of (4.7) is then

$$\epsilon_j(\theta, V/T) = K \star \sum_k N_{jk} \ln \left[1 + e^{-\mu_k/T} e^{\epsilon_k(\theta, V/T)} \right]. \quad (4.9)$$

The dependences on the mass ratios seems to have disappeared from (4.9), but they appear as an asymptotic condition: the original equations (4.7) indicates that the solution must satisfy

$$\epsilon_j \rightarrow \frac{m_j}{T} e^\theta \quad \text{as } \theta \rightarrow \infty.$$

We emphasize for later use that comparing the relations (4.7) and (4.5) gives

$$n_j(\theta, V) = \frac{T}{h} \partial_\theta \epsilon_j(\theta, V).$$

One effect of these equations is that the symmetry implies that

$$n_-(\theta, V) = n_+(\theta, V) \equiv n(\theta, V)$$

and $\epsilon_-(\theta, V) = \epsilon_+(\theta, V)$.

The analysis at general values of $1/\nu$ is more complicated. Since the bulk S matrix is not diagonal, the phase picked up when bringing a particle around the world can be expressed only as an eigenvalue of a monodromy matrix, which itself must be diagonalized. This can be done at the price of introducing a further Bethe ansatz (see [31,32] for example). The results are quite simple for $\nu/(1-\nu)$ integer: the equation (4.9) holds, with the addition of a term $\delta_{j1} M e^\theta / 2$ to the right-hand side. The general result is quite complicated, but the appropriate diagonalization has been done for all ν [29]. We caution that only for $1/\nu$ an odd integer does this one-component Luttinger liquid apply to the Hall effect; when ν is a more complicated fraction, the edge states of the quantum Hall effect may be described by models with more than one boson [4].

5. The current and the conductance

We have shown that the bosonic field theory with Hamiltonian (3.6) can be studied in terms of a particular set of quasiparticles and their scattering. We now compute an exact equation for the conductance using this basis.

Without the backscattering, the left and right charges (or equivalently, the even and odd charges) are conserved individually. The backscattering allows processes where a charge carrier of the left-moving edge hops to the right-moving edge or vice versa. In the original basis, the current I_B is the rate at which the charge of the left-moving edge is depleted. By symmetry, $\partial_t Q_L = -\partial_t Q_R$ in each such hopping event, so $I_B = \partial_t (\frac{e}{2} \Delta Q) = \partial_t (\frac{e}{\sqrt{2}} Q^o)$, and we see that in the even/odd basis, the tunneling corresponds to the violation

of odd charge conservation at the contact. In the S matrix language this happens when $S_{+-} \neq 0$, so that a particle of positive odd charge (the kink) can scatter into one of negative charge (the antikink) at the contact. Neutral quasiparticles cannot transport charge and thus do not directly contribute to $\partial_t \Delta Q$. We emphasize that neither the bulk nor the boundary S matrix elements depend on the voltage; the voltage only affects the thermodynamic properties.

To calculate the conductance, we start with a gas of quasiparticles with a chemical potential difference for kinks and antikinks corresponding to the voltage V . A positive voltage means that there are more kinks. When there are more kinks than antikinks, the backscattering will turn more kinks to antikinks than it turns antikinks to kinks. When a kink of momentum p is scattered into an antikink (the conservation laws require that it have the same momentum p) this changes ΔQ by -2 . Since kink and antikink quasiparticles scatter off the point contact one-by-one, we may describe the rate at which this charge transport occurs in terms of two quantities: the probabilities of finding a kink or antikink of momentum p at the contact, and the transition probability $|S_{+-}(\theta - \theta_B)|^2$. We therefore study the density of states $n(\theta, V) \equiv n_+(\theta, V) = n_-(\theta, V)$ and the distribution functions $f_{\pm}(\theta, V)$ in the thermodynamic limit ($l \rightarrow \infty$) and in the presence of an applied voltage V . We can now compute the backscattering current from a rate (Boltzmann) equation. The number density of kinks of rapidity θ which scatter into antikinks per unit time is given by $|S_{+-}|^2 n(\theta, V) \rho_{+-}$, where ρ_{+-} is the probability that the initial kink state of rapidity θ is filled *and* the final antikink state is empty. In a fermi liquid, we would have simply $\rho_{+-} = f_+[1 - f_-]$. However, in our interacting theory, correlations between the particles mean that this does not necessarily factorize in this manner. We can however write $\rho_{+-} = f_+ - f_{+-}$, where f_{+-} is the (unknown) probability that the kink and antikink state are *both occupied*. The rate at which antikinks scatter to kinks is likewise proportional to $\rho_{-+} = f_- - f_{+-}$. Thus the charge $Q_L - Q_R$ changes at a rate proportional to $\rho_{+-} - \rho_{-+} = f_+ - f_-$, independent of the unknown factor. Using (4.3) with $I_B = e \partial_t Q^o / \sqrt{2}$ gives

$$I_B(T_B, V, T) = -e \int_{-\infty}^{\infty} d\theta n(\theta) |S_{+-}(\theta - \theta_B)|^2 [f_+(\theta, V) - f_-(\theta, V)]. \quad (5.1)$$

Without the backscattering, the current is $I_0(V) = e \langle \Delta Q \rangle / 2l$, and it follows from (4.3) that I_0 is given by the same expression without the $-|S_{+-}|^2$. Thus the full current is

proportional to $1 - |S_{+-}|^2 = |S_{++}|^2$. Using the definition of f and the result $n(\theta) = \frac{T}{h} \partial_\theta \epsilon_\pm(\theta)$ allows us to simplify the resulting expression. Notice that

$$nf_\pm = -\frac{T}{h} \frac{\partial \epsilon_\pm}{\partial \theta} \frac{\partial}{\partial \epsilon_\pm} \ln(1 + e^{\pm eV/2T} e^{-\epsilon_\pm}) = -\frac{T}{h} \frac{\partial}{\partial \theta} \ln(1 + e^{\pm eV/2T} e^{-\epsilon_\pm})$$

Defining

$$\epsilon(\theta, V) \equiv \epsilon_+(\theta - \ln(M/2T), V) = \epsilon_-(\theta - \ln(M/2T), V)$$

and plugging into (5.1) gives our main result

$$\begin{aligned} I(T_B, V, T) &= \frac{eT}{h} \int_{-\infty}^{\infty} d\theta \frac{1}{1 + e^{2\lambda(\theta - \theta_B)}} \partial_\theta \ln \left[\frac{1 + e^{eV/2T} e^{-\epsilon(\theta + \ln(M/2T), V)}}{1 + e^{-eV/2T} e^{-\epsilon(\theta + \ln(M/2T), V)}} \right] \\ &= \frac{eT\lambda}{2h} \int_{-\infty}^{\infty} d\theta \frac{1}{\cosh^2[\lambda(\theta - \ln(T_B/T))]} \ln \left[\frac{1 + e^{eV/2T} e^{-\epsilon(\theta, V)}}{1 + e^{-eV/2T} e^{-\epsilon(\theta, V)}} \right] \end{aligned} \quad (5.2)$$

where to get to the second line we integrated by parts and redefined θ by a shift. Even though the breathers do not appear in (5.2), they interact with the kink and antikink and affect the calculation of ϵ .

The differential conductance is defined as $G(T_B/T, V/T) = \partial_V I(T_B, V, T)$. In the $V \rightarrow 0$ limit, the result can be written in a simple form. Using (4.7) and (4.5), it is easy to see that $d\epsilon/dV|_{V=0} = 0$, so [1]

$$G(T_B/T, 0) = \frac{e^2\lambda}{2h} \int_{-\infty}^{\infty} d\theta \frac{1}{1 + e^{\epsilon(\theta, 0)}} \frac{1}{\cosh^2[\lambda(\theta - \ln(T_B/T))]} \quad (5.3)$$

To check our result, we consider $\nu = 1/2$, where the conductance was previously derived exactly [5]. As noted above, the odd-boson kinks are simply free fermions [22,9,19], so they have the Fermi distribution function $f_\pm(\theta, V) = 1/[1 + \exp((Me^\theta \mp eV)/2T)]$ implying that the function $\epsilon(\theta)$ is simply $\epsilon(\theta) = e^\theta$. This of course follows from (4.7), because at $\nu = 1/2$ the bulk scattering is trivial and $\Phi_{jk} = 0$. Note again, as mentioned in Section 3.1 above, that we have used the kink/antikink description of the free fermion theory here, where all momenta have only *one* sign. Using the particle-hole transformation of Section 3.1, one finds immediately that the occupation number of kinks and antikinks are

$$f_\pm(p) = \Theta(p) \frac{1}{1 + e^{(p \mp V/2)/T}}, \quad p > 0, \quad \nu = \frac{1}{2}$$

whereas the occupation number of unoccupied kink/antikink states are

$$[1 - f_\pm](p) = \Theta(p) \frac{1}{1 + e^{(-p \pm V/2)/T}}, \quad p > 0, \quad \nu = \frac{1}{2}$$

Now all momenta have one sign. Note that $f_{\pm}(p=0, V=0) = 1/2$. These fermions (alias kinks) do scatter non-trivially off of the point contact, with S matrix given by (4.1). The resulting expression for $G(T_B, 0)$ obtained from (5.3) is identical to the result in sect. VIII of [5]. Actually one can re-express the integral in terms of dilogarithm functions after some lengthy but straightforward manipulations to find [33]

$$I(T_B, V, \nu = \frac{1}{2}) = \frac{e^2 V}{2h} \left[1 - \frac{2T_B}{eV} \text{Im} \psi \left(\frac{1}{2} + \frac{T_B}{2\pi T} + \frac{ieV}{4\pi T} \right) \right], \quad (5.4)$$

where the digamma function $\psi(x) = \Gamma'(x)/\Gamma(x)$. At zero voltage in particular one finds

$$G(T_B, 0, \nu = \frac{1}{2}) = \frac{e^2}{2h} \left[1 - \frac{T_B}{2\pi T} \psi' \left(\frac{1}{2} + \frac{T_B}{2\pi T} \right) \right], \quad (5.5)$$

and at zero temperature

$$I(V, \nu = \frac{1}{2}) = \frac{e^2 V}{2h} - \frac{eT_B}{h} \arctan \frac{eV}{2T_B}. \quad (5.6)$$

These $\nu = 1/2$ formulas also apply for ν near $1/2$ in the leading-logarithm approximation, after a V - and T -dependent renormalization of T_B [34].

Only at $T = 0$ can these equations be solved in closed form for all T_B ; we discuss this limit in the next subsection. However, we can study the solutions in certain limits. As $T_B/T \rightarrow 0$, we can evaluate the conductance explicitly, The linear-response conductance (5.3) becomes

$$G(0, 0) = [f_{\pm}(-\infty, 0) - f_{\pm}(\infty, 0)]e^2/h$$

in this limit. One finds $f_{\pm}(\infty, V) = 0$ obviously from (4.7) in this limit. More generally, one has

$$I(T_B = 0, V, T) = -\frac{eT}{h} \ln \left[1 - (1 - e^{-eV/T}) f_+(-\infty, V) \right]. \quad (5.7)$$

To find $f(0, V)$, we use a well-known trick, given for example in [11]. The kernels in (4.7) or (4.9) are appreciably different from zero only when θ' is near θ . Thus when we are interested in values of θ near $-\infty$, we can replace the value of $\epsilon(\theta', V)$ in the integral with $\epsilon(-\infty, V)$. We then can do the integral over the kernel explicitly. This then gives us the coupled difference equations

$$\epsilon_j(-\infty, V) = \sum_k \frac{N_{jk}}{2} \ln(1 + e^{-\mu_k/T} e^{\epsilon_k(-\infty, V)})$$

Solving these explicitly gives $f(-\infty, 0) = \nu$ and we indeed recover $G_0 = \nu e^2/h$. For the non-equilibrium conductance, it is not even obvious that G_0 will not depend on V . However, one can check that

$$f_+(-\infty, V) = \exp\left(\frac{eV(1-\nu)}{2T}\right) \frac{\sinh \nu eV/2T}{\sinh eV/2T}$$

and plugging this into (5.7) gives $G_0 = \nu e^2/h$ for all V .

These non-perturbative equations also give the perturbative exponents. As $T_B/T \rightarrow \infty$, the linear-response conductance $G \propto (T/T_B)^{2(1-\nu)/\nu}$. Thus it goes to zero with the correct exponent, as in [5]. For T_B/T small, it can be argued that $\epsilon(\theta + i\pi/(1-\nu)) = \epsilon(\theta)$ [30]. Using this to write a power series for ϵ and plugging into (5.2) gives $G - G_0 \propto (T_B/T)^{2(1-\nu)}$. Both are in agreement with [5]. In fact, when $\nu < 1/2$ all of the coefficients $g_n(V/T)$ in the series $G = \sum_{n=0}^{\infty} g_{2n}(T_B/T)^{2n(1-\nu)}$ can be computed using Jack polynomial technology [12]. Moreover, there is a non-perturbative functional relation [12] relating the linear-response conductance to the free energy for all $\nu < 1$.

We also note that there has been some confusion about the power of the exponent for T/T_B near zero. As discussed in [9], the leading (irrelevant) perturbation is the energy-momentum tensor, which is of scaling dimension two. This in fact means that the leading correction to the free energy is of order T^2 . (This power was also derived by scaling arguments in [35].) However, this operator does not give any contribution to the DC conductance. Intuitively, this is because the energy-momentum tensor has no charge and should not affect charge transport. More precisely, one can check that when inserted into the Kubo formula, powers of the frequency ω appear. When we take the DC $\omega \rightarrow 0$ limit this contribution vanishes. Thus the naive scaling arguments of [35] do not apply to the DC linear-response conductance. However, outside of linear response at $V > 0$, one finds indeed that

$$I(T_B, V, T) \approx I(T_B, V, 0) + T^2 I_2(T_B, V) + \dots$$

in agreement with [34,35].

We can easily solve for the conductance numerically. To plot the complete function, one fixes a value of V/T and solves (4.7) numerically for ϵ to double-precision accuracy and inserts the result into (5.2). Evaluating the integral numerically for various values of T/T_B then gives $I(T_B/T, V/T)/V$ as a function of T_B for fixed V and T . To find the conductance it is easiest to just vary the voltage slightly in order to take the derivative numerically. A more precise way would be to use the fact that once one knows ϵ numerically, the integral

equations for $d\epsilon/dV$ are linear and can be solved by inverting large matrices (of size the number of lattice sites used in the discretization of the integral) numerically.

Several graphs of G for $\nu = 1/3$ are given in the figures. For $V/T < 8$, the plot is qualitatively the same as for $V = 0$: a flat region at $G = e^2/3h$ for T large, a transition region where the power series corrections cause it to fall off until it reaches its asymptotic form proportional to $(T/T_B)^4$. However, at $V/T \approx 8$, a qualitatively new feature appears: G has a peak! It is not very sharp; the highest it gets for $\nu = 1/3$ is $G \approx .35e^2/h$. A variety of values of V/T are plotted in fig. 1 and fig. 2. In the first we plot it versus T_B/V in order to make the approach to the $T = 0$ limit to be discussed in sect. 6 clear. In the second we plot it versus T_B/T ; we see that there is a substantial broadening of the curve as the voltage is increased. This should provide a prominent signal in the experiments.

This peak and the values of V/T for which it occurs can be understood theoretically. A peak occurs for voltages large enough so that $g_2(V/T)$ changes sign. This must happen because at zero temperature the current can be expanded for large voltage in the form

$$I(V) \propto V(\nu + C \left(\frac{T_B}{V}\right)^{2(1-\nu)} + \dots)$$

Because the backscattering must make the current decrease we have $C < 0$. Taking the derivative with respect to V we see that for $\nu < 1/2$ the conductance must increase for small enough V/T_B . We can even find the value V^* where $g_2(V^*/T) = 0$ analytically, because g_2 can be calculated in closed form [12]. This is done by first calculating the coefficient Z_2 of the partition function in the case where the interaction (in Euclidean time) is $\cos[\sqrt{2}\phi(0, \tau) + 2\pi p\tau T]$, which is [12]

$$Z_2(p) = \frac{\sin \pi \nu \Gamma(1 - 2\nu)}{\sin \pi(\nu + p)\Gamma(1 - \nu + p)\Gamma(1 - \nu - p)}.$$

The finite voltage case is obtained by analytically continuing $2\pi p$ to $i\nu eV/T$ [5]. Then we use the relation $g_2(V/T) \propto \text{Re} \partial_p Z_2(p)$ (which can be shown by using explicit perturbation theory in the impurity interaction) to give

$$g_2(V/T) \propto \text{Re} \left[Z_2 \left(\frac{i\nu eV}{2\pi T} \right) \left\{ \psi\left(\nu + \frac{i\nu eV}{2\pi T}\right) - \psi\left(1 - \nu + \frac{i\nu eV}{2\pi T}\right) \right\} \right]. \quad (5.8)$$

Solving for $g_2(V^*/T) = 0$ gives $eV^*/T = 7.18868564374998\dots$ for $\nu = 1/3$ and $eV^*/T = 6.653022289582846\dots$ for $\nu = 1/4$.

The perturbative results of [12] give a completely independent check on the TBA results. One can fit the TBA results to a power series numerically to determine the perturbative coefficients to compare; one indeed finds for example that $g_2(V^*/T) = 0$ in the TBA results. One can also check that the relation $T_B = C\lambda_1^{1/1-\nu}$ is independent of V , showing that the boundary S matrix is indeed independent of voltage.

6. Explicit Solution at $T=0$

Some remarkable simplifications take place in the $T = 0$ limit. Although the densities of states are still non-trivial, the distribution functions f become step functions. As a result, the TBA equations become linear and can be solved using the Wiener-Hopf technique. We find explicit series expressions for $I(V/T_B)$ and $G(V/T_B)$ in this limit. Moreover, this leads to an exact duality between large V/T_B and small V/T_B . In the Hall devices this corresponds to a duality between Laughlin-quasiparticle tunneling and electron tunneling.

At $T = 0$ and $V = 0$ the ground state of the theory is just the vacuum with neither kinks nor breathers; these particles are in fact defined as excitations above this vacuum. When V is turned on, this ground state becomes unstable. For $V > 0$, kinks of charge e start filling the vacuum, since they are energetically favorable for small enough momentum (large negative rapidity). The new ground state is made of kinks occupying the range $\theta \in (-\infty, A]$; in other words, $f_+(\theta, V) = 1$ for $\theta < A$ and $f_+(\theta, V) = 0$ for $\theta > A$. The surface of the sea is approximately $A \approx \ln(eV/M)$, but computing A exactly requires some technology because the kink interaction affects the filling of the sea. There are no antikinks nor breathers in the sea at $T = 0$, so their densities do not appear in this analysis. For ease of notation we define $\rho(\theta) \equiv n_+(\theta, V)f_+(\theta, V)|_{T=0}$. When $T = 0$ the periodicity relation (4.5) reduces to the following coupling between kink rapidities:

$$2\pi n_+(\theta) = \frac{M}{2\hbar} e^\theta + 2\pi \int_{-\infty}^A \Phi(\theta - \theta') \rho(\theta') d\theta', \quad (6.1)$$

where $\rho = 0$ in $[A, \infty)$, and $\Phi = \partial_\theta S_{++}(\theta)/2\pi$ follows from the kink-kink bulk S matrix (4.2).

We consider now the general equation

$$\rho(\theta) - \int_{-\infty}^A \Phi(\theta - \theta') \rho(\theta') d\theta' = g(\theta), \quad \theta \in (-\infty, A], \quad (6.2)$$

where in the above example $g(\theta) = \frac{M}{2\hbar} e^\theta$ for $\theta \in (-\infty, A]$, $g(\theta) = 0$ otherwise. By taking Fourier transforms, and since ρ vanishes outside $(-\infty, A]$ we have

$$\int_{-\infty}^{\infty} d\omega e^{-i\omega\theta} \left\{ \tilde{\rho}(\omega) [1 - \tilde{\Phi}(\omega)] - \tilde{g}(\omega) \right\} = 0, \quad \theta \in (-\infty, A], \quad (6.3)$$

where we defined Fourier transforms by

$$\tilde{h}(\omega) = \int h(\theta) e^{i\omega\theta} d\theta, \quad h(\theta) = \int \tilde{h}(\omega) e^{-i\omega\theta} \frac{d\omega}{2\pi}.$$

For any function h we also introduce

$$h_-(\omega) \equiv \tilde{h}(\omega)e^{-i\omega A}.$$

This subscript should not be confused with the antikink index used in other sections of this paper.

The integral equation (6.2) for ρ can now be written in the form

$$\tilde{\rho}(1 - \tilde{\Phi}) - \tilde{g} = e^{i\omega A} X_+(\omega), \quad (6.4)$$

where $X_+(\omega)$ is analytic in the upper half plane. Since ρ vanishes in $[A, \infty)$ we see that ρ_- is analytic in the lower half plane, and similarly for g_- . To implement the Wiener-Hopf technique (see the appendix in [36] for a very clear exposition), we need to factorize $1 - \tilde{\Phi}$ into the form

$$1 - \tilde{\Phi} = \frac{\sinh[(\lambda + 1)\pi\omega/2\lambda]}{2 \cosh[\pi\omega/2] \sinh[\pi\omega/2\lambda]} \equiv \frac{1}{G_+ G_-}, \quad (6.5)$$

where $G_+(G_-)$ is analytic in the upper (resp. lower) half plane and $G_+(G_-)$ vanishes only in the lower (resp. upper) half plane. One finds

$$G_+ = \sqrt{2\pi(\lambda + 1)} \frac{\Gamma(-i(1 + \lambda)\omega/2\lambda)}{\Gamma(-i\omega/2\lambda)\Gamma(1/2 - i\omega/2)} e^{-i\omega\Delta}, \quad (6.6)$$

$$G_-(\omega) = G_+(-\omega),$$

$$\Delta \equiv \frac{1}{2} \ln \lambda - \frac{1 + \lambda}{2\lambda} \ln(1 + \lambda).$$

The phase ensures analyticity of G_+ at $i\infty$. Having set up the equation in this form, we can write down the solution for ρ :

$$\frac{\rho_-}{G_-} = [g_- G_+]_-, \quad (6.7)$$

where

$$[h]_-(\omega) \equiv -\frac{1}{2i\pi} \int_{-\infty}^{\infty} \frac{h(\omega')}{\omega' - \omega + i0} d\omega'.$$

In our case

$$\tilde{g}(\omega) = \frac{M}{2h} \frac{e^{(i\omega+1)A}}{i\omega + 1},$$

so we find

$$\tilde{\rho}(\omega) = \frac{M}{2ih} \frac{G_-(\omega)G_+(i)}{\omega - i} e^{(i\omega+1)A}. \quad (6.8)$$

This relation was obtained also in [37].

We have not yet determined the dependence of the cut-off A on the physical potential V . This can be done in two ways. The first way consists in minimizing the energy of the system. Following [38] we introduce a function $\epsilon(\theta)$ which satisfies

$$\frac{eV}{2} - \frac{M}{2}e^\theta = \epsilon(\theta) - \int_{-\infty}^A \Phi(\theta - \theta')\epsilon(\theta')d\theta', \quad (6.9)$$

and the cut-off follows now from the condition $\epsilon(A) = 0$, which reads in terms of fourier transforms

$$\lim_{\omega \rightarrow \infty} \omega \epsilon_-(i\omega) = 0.$$

We can easily solve for ϵ . This is the same equation as the one for ρ except for the substitution

$$g(\theta) = \frac{eV}{2} - \frac{M}{2}e^\theta, \quad \tilde{g}(\omega) = \pi eV \delta(\omega) - \frac{M}{2} \frac{e^{(i\omega+1)A}}{i\omega + 1}.$$

We find therefore

$$\epsilon_-(\omega) = -\frac{M}{2i} \frac{G_-(\omega)G_+(i)}{\omega - i} e^A + \frac{eV}{2i} \frac{G_-(\omega)G_+(0)}{\omega}. \quad (6.10)$$

It follows that

$$e^A = \frac{eV}{M} \frac{G_+(0)}{G_+(i)}. \quad (6.11)$$

The second method of determining A is to study the energy in the absence of backscattering, which is

$$\begin{aligned} E &= \int_{-\infty}^A d\theta \rho(\theta) \left[\frac{M}{2}e^\theta - \frac{eV}{2} \right] = \frac{M}{2} \tilde{\rho}(-i) - \frac{eV}{2} \tilde{\rho}(0) \\ &= \frac{M^2}{8h} G_+(i)G_-(-i)e^{2A} - \frac{eM}{4h} G_-(0)G_+(i)V e^A. \end{aligned}$$

This energy results from the massless description obtained by considering the free field as the $\lambda \rightarrow 0$ limit of the sine-Gordon model (3.6). We can recover this energy directly from the Hamiltonian in this limit. Coupling to a potential amounts to considering the Hamiltonian (in the original left-right basis)

$$H_0 = \frac{\hbar}{4\pi\nu} \int_{-l}^l dx [(\partial_x \varphi_R)^2 + (\partial_x \varphi_L)^2] - \frac{eV}{4\pi} \int_{-l}^l dx [\partial_x \varphi_L + \partial_x \varphi_R]. \quad (6.12)$$

Redefining the fields ϕ_L and ϕ_R by a shift removes the linear term, and gives the energy per unit length associated with the potential V . Equating the two energies gives A in agreement with formula (6.11).

Since we know the density explicitly from (6.8) and (6.11), an explicit form for the current follows from (5.1), which at $T = 0$ reads

$$\begin{aligned} I(V, T_B) &= e \int_{-\infty}^A \rho(\theta) |S_{++}(\theta - \theta_B)|^2 d\theta \\ &= \frac{e^2 V}{2h} \int_{-\infty}^0 d\theta F(\theta) \frac{1}{1 + \exp[-2\lambda(\theta + \ln(eV/T'_B) - \Delta)]}. \end{aligned} \quad (6.13)$$

where

$$\tilde{F}(\omega) \equiv \frac{G_-(\omega)G_+(0)}{1 + i\omega},$$

and the boundary temperature is redefined:

$$T'_B \equiv T_B 2e^{-\Delta} \frac{G_+(i)}{G_+(0)} = T_B \frac{2\sqrt{\pi}(\lambda + 1)\Gamma(\frac{1}{2} + \frac{1}{2\lambda})}{\Gamma(\frac{1}{2\lambda})}.$$

We can therefore extract the following results from (6.13). At very large potential, the S matrix element goes to one and $I_0 = G_0 V$, with

$$G_0 = \frac{e^2}{2h} \int_{-\infty}^0 F(\theta) d\theta = \frac{e^2 \nu}{h}. \quad (6.14)$$

For small voltage, we can expand the S matrix element in powers of V/T'_B to get

$$\begin{aligned} I(V, T_B) &= \frac{e^2 V}{2h} \int_{-\infty}^0 F(\theta) d\theta \sum_{n=1}^{\infty} (-1)^{n+1} \left(\frac{eV}{T'_B} e^{\theta} \right)^{2n\lambda} \\ &\equiv \frac{e^2 V}{2h} \sum_{n=1}^{\infty} I_{2n} \left(\frac{eV}{T'_B e^{\Delta}} \right)^{2n\lambda}, \end{aligned} \quad (6.15)$$

where

$$I_{2n} = \frac{(-1)^{n+1}}{2\pi} \int_{-\infty}^{\infty} \frac{G_-(\omega)G_+(0)}{(1 + i\omega)(2n\lambda - i\omega)} d\omega = (-1)^{n+1} \frac{G_-[-2in\lambda]G_+(0)}{1 + 2n\lambda}.$$

This expansion is valid only for $eV e^{-\Delta}/T'_B < 1$. By using (6.6), we find our final result for the low-voltage expansion

$$I = \frac{e^2}{h} V \sum_{n=1}^{\infty} (-1)^{n+1} \frac{\sqrt{\pi} \Gamma(\frac{n}{\nu})}{2\Gamma(n)\Gamma(\frac{3}{2} + n(\frac{1}{\nu} - 1))} \left(\frac{eV}{T'_B} \right)^{2n(\frac{1}{\nu} - 1)}, \quad \frac{eV}{T'_B e^{\Delta}} < 1. \quad (6.16)$$

We prove in the appendix that this strong-barrier expansion can be transformed into the following weak-barrier expansion

$$I = \frac{e^2 V \nu}{h} \left[1 - \sum_{n=1}^{\infty} (-1)^{n+1} \frac{\nu \sqrt{\pi} \Gamma(n\nu)}{2\Gamma(n)\Gamma(\frac{3}{2} + n(\nu - 1))} \left(\frac{eV}{T'_B} \right)^{2n(\nu-1)} \right], \quad \frac{eV}{T'_B e^{\Delta}} > 1. \quad (6.17)$$

Up to a constant and a shift, this is the same expression as for strong backscattering, with the replacement $\nu \rightarrow \frac{1}{\nu}$. We therefore have the result

$$I(T'_B, V, \nu) = \frac{e^2 \nu V}{h} - \nu^2 I(T'_B, V, \frac{1}{\nu}). \quad (6.18)$$

(In this equation, T'_B is treated as a constant — it is the same on both sides, although we have seen T'_B/T_B depends on ν .) This proves that for $T = 0$ at least, the weak-barrier (small T_B) and strong-barrier (large T_B) are completely dual to each other. In the Hall device, this duality is a concrete proof of a long-suspected relation between electrons and Laughlin quasiparticles. This arises from the fact that for weak backscattering, the operator for the tunneling of Laughlin quasiparticles is relevant while the electron tunneling operator is always irrelevant [4,5]. Laughlin quasiparticles are allowed to tunnel because they are tunneling through the bulk of the sample. However, in the strong backscattering limit, only electrons can tunnel because they are not tunneling through the Hall fluid. Thus the least irrelevant operator arises from electron tunneling. As seen in [5], the associated exponents are indeed related by duality; we find here that the entire expansions around these two limits are related.

This duality was somehow known in the literature [39], but its status is not totally clear to us. It is usually considered as only approximate since it relies on an instanton approximation in the large-barrier limit [5]. However, one can prove an exact duality [40] (in the context of dissipative quantum mechanics, which is equivalent) between the cosine problem in the UV and the “tight-binding” problem in the zero-temperature limit, and then in [41] the tight-binding problem is mapped back onto the cosine problem, providing a sort of proof. The main source of difficulty is that the zero-temperature action must be handled with great care. Perturbation theory around the zero-temperature fixed point is ill-behaved and depends on an infinite number of counterterms (see the discussion at the end of [31] in the case of the flow from tricritical Ising to Ising model), so identifying the leading term in the approach to this fixed point is not sufficient. This is equivalent to saying that what one calls the strong-barrier problem must actually be defined with

great care. The strong-barrier problem which is at the end of our renormalization-group trajectory follows formally from dimensional continuation of the integrals for the weak barrier problem. It is not in any case a generic strong-barrier problem. For instance regularizing the integrals with a short-distance cut-off would give very different results, with a non-monotonic conductance [40]. Also, note that the duality does not apply to the impurity free energy, for example as explained in [9] for small T the leading contribution is proportional to T^2 for all ν .

Interestingly (6.17) can be compared with the perturbative expansion in [5]

$$I(V) = \frac{e^2 \nu V}{h} \left[1 - \frac{\pi^2 \nu}{\Gamma(2\nu)} (eV\nu)^{2(\nu-1)} (2\lambda_1 \kappa^{-\nu})^2 \right], \quad (6.19)$$

thus providing the relation between the parameter λ_1 in the action and the TBA parameter T_B :

$$\lambda_1 \kappa^{-\nu} = \frac{2^\nu}{4\pi} \Gamma(\nu) (\nu T'_B)^{1-\nu}. \quad (6.20)$$

where κ is the non-universal (dimensionful) cutoff which appears in the boson two-point function, as defined in [12].

Finally, setting $\nu = \frac{1}{2}$ (i.e. $\lambda = 1$) in these formulas gives $G_+(in) = 1$ so $I_n = \frac{(-1)^{n+1}}{2n+1}$ and $T'_B = 4T_B$. Hence

$$I(V) = \frac{e^2 V}{2h} \sum_{n=1}^{\infty} \frac{(-1)^{n+1}}{2n+1} \left(\frac{eV}{T_B} \right)^{2n} = \frac{e^2 V}{2h} - \frac{eT_B}{h} \arctan \frac{eV}{2T_B},$$

in agreement with the $T \rightarrow 0$ limit of eq (5.4).

Acknowledgements:

We thank the many participants of the conference SMQFT (May '94, USC) for discussions, and more particularly I. Affleck, M.P.A. Fisher, F.D.M. Haldane, N.P. Warner and E. Wong. We also thank D. Freed, C. Mak and F.P. Milliken for valuable input. This work was supported by the Packard Foundation, the National Young Investigator program (NSF-PHY-9357207) and the DOE (DE-FG03-84ER40168), as well as by a Sloan Foundation Fellowship (A.W.W.L).

Appendix A. Duality

In this appendix we provide details of the derivation of duality between strong- and weak-tunneling regimes. Defining

$$b = \left(\frac{T'_B e^\Delta}{eV} \right)^{2(\frac{1}{\nu}-1)},$$

we see that there are two different regions to consider in the computation of the integral

$$\int_{-\infty}^0 \frac{e^{-i\omega\theta}}{1 + be^{-2(\frac{1}{\nu}-1)\theta}}$$

depending on whether $be^{-2(\frac{1}{\nu}-1)\theta}$ is greater or smaller than one. In each region, one can expand the integrand appropriately, and integrate term by term. For V/T_B small, this piece is always smaller than one, and the expansion (6.15) follows immediately. For V/T_B large, one divides the integral in (6.13) into two pieces to get

$$\begin{aligned} I(V) = & \frac{e^2 V}{2h} PP \int_{-\infty}^{\infty} \frac{d\omega}{2\pi} \frac{G_-(\omega)G_+(0)}{1+i\omega} \left\{ \sum_{N=0}^{\infty} (-1)^{N+1} \frac{b^{2N}}{i\omega + 2(\frac{1}{\nu}-1)N} \right. \\ & \left. + b^{-i\omega/(2(\frac{1}{\nu}-1))} \sum_{N=0}^{\infty} \left[\frac{(-1)^N}{i\omega + 2(\frac{1}{\nu}-1)N} + \frac{(-1)^N}{-i\omega + 2(\frac{1}{\nu}-1)(N+1)} \right] \right\}. \end{aligned} \quad (\text{A.1})$$

The poles of the rational functions except the one for $\omega = 0$ are all cancelled out because $G_-(2N(\frac{1}{\nu}-1)i) = 0$ for $N > 0$. For the first sum we close the contour in the lower half plane. Since G_- is regular in this regime, the only pole is at $\omega = 0$. For the second sum we close the contour in the upper half plane where there are poles of $G_-(\omega)$ at

$$\omega = 2in(\nu-1), \quad n > 0.$$

as well as those of the rational function at $\omega = 0$. Collecting all terms gives

$$I(V) = \frac{e^2 V}{2h} \left\{ 2\nu + 4\sqrt{\pi}(\nu - 1) \sum_{n>0} (-1)^n \frac{1}{1 + 2n(\nu - 1)} \frac{1}{\Gamma(-n\nu)\Gamma(1/2 + n(\nu - 1))} \right. \\ \left. \frac{1}{2(\frac{1}{\nu} - 1)} \left(\frac{T'_B}{eV} \right)^{2n(1-\nu)} \sum_{N=0}^{\infty} \left[\frac{(-1)^N}{N - n\nu} + \frac{(-1)^N}{(N + 1) + n\nu} \right] \right\}. \quad (\text{A.2})$$

Using the identity

$$\sum_{N=0}^{\infty} \frac{(-1)^N}{N - n\nu} + \frac{(-1)^N}{N + 1 + n\nu} = -\frac{\pi}{\sin \pi n\nu}$$

together with standard gamma-function identities gives (6.17).

Appendix B. Incidence Matrix

In this appendix we give some details involving the manipulations of the “incidence matrix” of section 4, for the case $\nu = 1/3$. We start by writing

$$\Phi(\theta) \equiv \begin{pmatrix} \Phi_{++} & \Phi_{+b} & \Phi_{+-} \\ \Phi_{b+} & \Phi_{bb} & \Phi_{b-} \\ \Phi_{-+} & \Phi_{-b} & \Phi_{--} \end{pmatrix}(\theta)$$

Using the explicit expressions given in (4.6), one finds that this may be written in the form

$$\Phi(\theta) \equiv \Phi_{++}(\theta)\mathbf{N}^2 + \Phi_{+b}(\theta)\mathbf{N}$$

where

$$\mathbf{N} \equiv \begin{pmatrix} 0 & 1 & 0 \\ 1 & 0 & 1 \\ 0 & 1 & 0 \end{pmatrix}$$

It is convenient to fourier transform the rapidity dependence, in order to turn convolutions into multiplications. We find

$$\tilde{\Phi}_{++}(k) = \int_{-\infty}^{\infty} d\theta e^{ik\theta} \Phi_{++}(\theta) = -\frac{1}{2 \cosh(k\pi/2)}$$

$$\tilde{\Phi}_{+b}(k) = \int_{-\infty}^{\infty} d\theta e^{ik\theta} \Phi_{+b}(\theta) = -\frac{\cosh(k\pi/4)}{\cosh(k\pi/2)}$$

Making use of the relation $\mathbf{N}^3 = 2\mathbf{N}$, we find in fourier space

$$\mathbf{N} \cdot \tilde{\Phi}(k) = \tilde{\Phi}_{+b}(k)\mathbf{N}^2 + 2\tilde{\Phi}_{++}(k)\mathbf{N}$$

If we define the multiplicative factor

$$\tilde{K}(k) = \tilde{\Phi}_{++}(k)/\tilde{\Phi}_{+b}(k) = \frac{1}{2 \cosh(k\pi/4)}$$

we find

$$\tilde{K}\mathbf{N} \cdot \tilde{\Phi} = \tilde{\Phi} + (2\tilde{K}\tilde{\Phi}_{++} - \tilde{\Phi}_{+b})\mathbf{N}$$

The expression in parenthesis equals $(2\tilde{K}\tilde{\Phi}_{++} - \tilde{\Phi}_{+b}) = 1/(2 \cosh(k\pi/4)) = K(k)$. In conclusion we have found

$$\tilde{K}\mathbf{N} \cdot \tilde{\Phi} = \tilde{\Phi} + \tilde{K}\mathbf{N}. \quad (\text{B.1})$$

Fourier-transforming back to rapidity space, we find the relation (4.8) of section 4. Note that for $\nu = 1/3$,

$$K(\theta) = \int_{-\infty}^{\infty} \frac{dk}{2\pi} e^{-ik\theta} \tilde{K}(k) = \frac{1}{\pi \cosh(2\theta)}$$

as indicated below (4.8).

References

- [1] P. Fendley, A. Ludwig and H. Saleur, Phys. Rev. Lett. 74 (1995) 3005, cond-mat/9408068.
- [2] F.P. Milliken, C.P. Umbach and R.A. Webb, “Indications of a Luttinger Liquid in the Fractional Quantum Hall Regime”, to appear in Solid State Communications.
- [3] F.D.M. Haldane, J. Phys. C14 (1981) 2585.
- [4] X.G. Wen, Phys. Rev. B41 (1990) 12838; Phys. Rev. B43 (1991) 11025.
- [5] C.L. Kane and M.P.A. Fisher, Phys. Rev. B46 (1992) 15233.
- [6] K. Moon, H. Yi, C.L. Kane, S.M. Girvin and M.P.A. Fisher, Phys. Rev. Lett. 71 (1993) 4381.
- [7] W. Apel and T.M. Rice, Phys. Rev. B26 (1982) 7063.
- [8] S. Ghoshal and A.B. Zamolodchikov, Int. J. Mod. Phys. A9 (1994) 3841, hep-th/9306002.
- [9] P. Fendley, H. Saleur and N.P. Warner, Nucl. Phys. B430 (1994) 577, hep-th/9406125.
- [10] C.N. Yang and C.P. Yang, J. Math. Phys. 10 (1969) 1115
- [11] A.B. Zamolodchikov, Nucl. Phys. B342 (1991) 695.
- [12] P. Fendley, F. Lesage and H. Saleur, J. Stat. Phys. 79 (1995) 799, hep-th/9409176.
- [13] C. Kane and M.P.A. Fisher, Phys. Rev. B 46 (1992) 7268.
- [14] A. Luther and I. Peschel, Phys. Rev. B12 (1975) 3908;
S. Coleman, Phys. Rev. D11 (1975) 2088.
- [15] for a review of this method, see I. Affleck in Les Houches 1988 *Fields, strings, and critical phenomena*, ed. by E. Brézin and J. Zinn-Justin (North-Holland, 1990).
- [16] M. Stone and M.P.A. Fisher, Int. J. Mod. Phys. B8 (1994) 2539, cond-mat/9402040.
- [17] C.G. Callan and I.R. Klebanov, Phys. Rev. Lett. 72 (1994) 1968, hep-th/9311092; C.G. Callan, I. Klebanov, A.W.W. Ludwig and J. Maldacena, Nucl. Phys. B422 (1994) 417, hep-th/9402113; J. Polchinski and L. Thorlacius, Phys. Rev. D50 (1994) 622, hep-th/9404008.
- [18] E. Wong and I. Affleck, Nucl. Phys. B417 (1994) 403, cond-mat/9311040.
- [19] I. Affleck and A.W.W. Ludwig, J. Phys. A27 (1994) 5375, cond-mat/9405057.
- [20] N. Andrei, K. Furuya, and J. Lowenstein, Rev. Mod. Phys. 55 (1983) 331;
A.M. Tsvelick and P.B. Wiegmann, Adv. Phys. 32 (1983) 453.
- [21] B.M. McCoy and T.T. Wu, Nuovo Cimento 56B (1968) 311.
- [22] F. Guinea, Phys. Rev. B32 (1985) 7518.
- [23] A.M. Polyakov, Phys. Lett. 72B (1977) 224.
- [24] A.B. Zamolodchikov and A.I. Zamolodchikov, Ann. Phys. 120 (1979) 253.
- [25] L.D. Faddeev and L.A. Takhtajan, Phys. Lett. A85 (1981) 375.
- [26] N.Yu. Reshetikhin and H. Saleur, Nucl. Phys. B419 (1994) 507.
- [27] F.D.M. Haldane, Phys. Rev. Lett. 67 (1991) 937.

- [28] T.R. Klassen and E. Melzer, Nucl. Phys. B338 (1990) 485.
- [29] M. Takahashi and M. Suzuki, Prog. Th. Phys. 48 (1972) 2187.
- [30] Al.B. Zamolodchikov, Phys. Lett. B253 (1991) 391.
- [31] Al. B. Zamolodchikov, Nucl. Phys. B358 (1991) 497.
- [32] P. Fendley and K. Intriligator, Nucl. Phys. 372 (1992) 533.
- [33] U. Weiss, M. Sassetti, T. Negele and M. Wollensak, Z. Phys. B 84 (1991) 471.
- [34] U. Weiss, R. Egger and M. Sassetti, “Low-temperature nonequilibrium transport in a Luttinger liquid”, to appear in Phys. Rev. B.
- [35] F. Guinea, G. Gomez Santos, M. Sassetti and M. Ueda, “Asymptotic tunneling conductance in Luttinger liquids”, cond-mat/9411130.
- [36] G. Japaridze, A. Nersesyan and P. Wiegmann, Nucl. Phys. B230 (1984) 511.
- [37] A.M. Tsvelick, “Capacitance and transport through an isolated impurity in one-dimensional Luttinger liquid”, cond-mat/9409027.
- [38] P. Fendley, H. Saleur and Al.B. Zamolodchikov, Int. J. Mod. Phys. A8 (1993) 5751.
- [39] A. Schmid, Phys. Rev. Lett. 51 (1983) 1506.
- [40] M.P.A. Fisher and W. Zwerger, Phys. Rev. B32 (1985) 6190.
- [41] F. Guinea, V. Hakim and A. Muramatsu, Phys. Rev. Lett. 54 (1985) 263.

Figure Captions

Fig. 1 . The non-equilibrium conductance as a function of $\log(T_B/V)$, for various values of V/T . Notice that the curve develops a peak when $V/T > 7.18868$, and that the $T \rightarrow 0$ limit is smooth.

Fig. 2. The non-equilibrium conductance as a function of T_B/T for various values of V/T . The curve broadens substantially as V/T is increased, even before developing a peak.

